

AD-A104 566

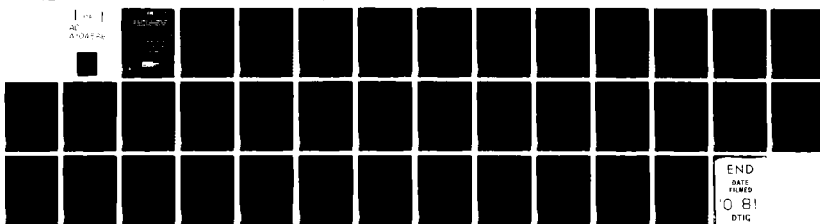
UNITED TECHNOLOGIES RESEARCH CENTER EAST HARTFORD CT
DEVELOPMENT OF A PREDICTION METHOD FOR TRANSONIC SHOCK INDUCED --ETC(U)
SEP 81 J E CARTER
N00014-80-C-0424

UNCLASSIFIED

UTRC/R80-915213-4

F/G 20/4

NL



END
DATE FILMED
10.81
DTIG

R80-815213-4

LEVEL ✓

12

ADA104566

DEVELOPMENT OF A PREDICTION METHOD FOR TRANSONIC SHOCK INDUCED SEPARATED FLOW

J.E. Carter

Final Report
May, 1980 - March, 1981



Under Contract No. N00014-80-C-0424

for
Office of Naval Research
Arlington, Va.

FILE COPY



81 9 25 065

(14) UTRC/R80-915213-4

REPORT DOCUMENTATION PAGE		READ INSTRUCTIONS BEFORE COMPLETING FORM	
1. REPORT NUMBER R80-915213-4	2. GOVT ACCESSION NO. AD-A304	3. RECIPIENT'S CATALOG NUMBER (9)	
4. TITLE (and SUBTITLE) Development of a Prediction Method for Transonic Shock Induced Separated Flow.		5. TYPE OF REPORT & PERIOD COVERED Final Report May 1980 - March 1981	
6. AUTHOR(s) J. E. Carter		7. PERFORMING ORGANIZATION REPORT NUMBER UTRC Report R80-915213-4	
8. CONTRACT OR GRANT NUMBER(s) N00014-80-C-0424		9. PERFORMING ORGANIZATION NAME AND ADDRESS United Technologies Research Center Silver Lane East Hartford, CT 06108	
10. PROGRAM ELEMENT, PROJECT, TASK AREA & WORK UNIT NUMBERS		11. CONTROLLING OFFICE NAME AND ADDRESS Office of Naval Research 800 N. Quincy Street Arlington, VA 22217	
12. REPORT DATE Sep 1 1981		13. NUMBER OF PAGES 38	
14. MONITORING AGENCY NAME & ADDRESS (if different from Controlling Office)		15. SECURITY CLASS. (of this report) Unclassified	
16. DISTRIBUTION STATEMENT (of this Report)		17. DECLASSIFICATION/DOWNGRADING SCHEDULE	
Approved for public release; distribution unlimited			
18. SUPPLEMENTARY NOTES			
19. KEY WORDS (Continue on reverse side if necessary and identify by block number) Transonic shock wave boundary - layer interaction; viscous - inviscid iteration; separated flow; inverse boundary-layer			
20. ABSTRACT (Continue on reverse side if necessary and identify by block number) In the present study it has been demonstrated that a finite difference technique for viscous-inviscid interaction, previously developed and demonstrated by the author for subsonic turbulent separated flows, is applicable to the problem of transonic shock induced separated flow. Converged solutions have been obtained and favorable comparisons with experimental data show that this method is capable of resolving the detailed features of this strongly interacting flow. These interaction			

SECURITY CLASSIFICATION OF THIS PAGE (When Data Entered)

calculations are aided by the use of a new shear layer coordinate system which is aligned with an estimated position of the shear layer in the large separated region.

S/N 0102-LF-014-6601

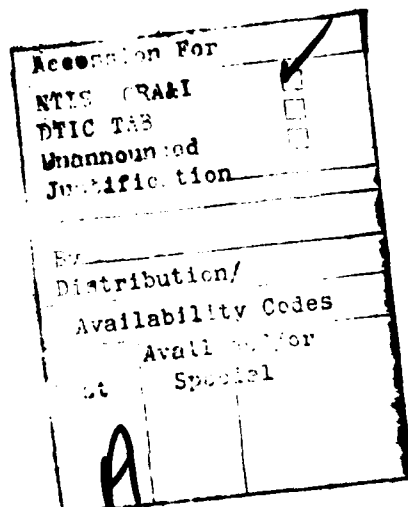
SECURITY CLASSIFICATION OF THIS PAGE(When Data Entered)

R80-915213-4

Development of a Prediction Method for Transonic
Shock Induced Separated Flow

TABLE OF CONTENTS

	<u>Page</u>
SUMMARY	1
INTRODUCTION	2
ANALYSIS	3
Shear Layer Coordinate System	3
Inverse Boundary Layer Procedure.	3
Inviscid Analysis	6
Viscous-Inviscid Iteration.	7
RESULTS AND DISCUSSION	8
Upstream Boundary Layer Analysis.	8
Comparison with Experiment.	9
CONCLUDING REMARKS	13
REFERENCES	
FIGURES	



R80-915213-4

FOREWORD

This report covers the work supported under ONR Contract No. N00014-80-C-0424 and constitutes the final report under that contract. This represents an interim report on an overall technical effort on transonic shock induced separated flow which is currently being continued under ONR Contract No. N00014-81-C-0381.

SUMMARY

In the present study it has been demonstrated that a finite difference technique for viscous-inviscid interaction, previously developed and demonstrated by the author for subsonic turbulent separated flows, is applicable to the problem of transonic shock induced separated flow. Converged solutions have been obtained and favorable comparisons with experimental data show that this method is capable of resolving the detailed features of this strongly interacting flow. These interaction calculations are aided by the use of a new shear layer coordinate system which is aligned with an estimated position of the shear layer in the large separated region.

INTRODUCTION

The prediction of transonic shock induced separated flow represents a formidable, but important problem in aerodynamics because of the frequent occurrence of this phenomena in many types of configurations. Examples include airfoils in supercritical flow - both external and internal (turbo-machinery applications), exhaust nozzles, and engine inlets. The presence of separated flow often results in an overly conservative aerodynamic design due to our current inability to accurately predict such flows, even in cases where the separated region is small. In the last few years, there have been significant advances in the development of viscous-inviscid interaction techniques as demonstrated by the recent AGARD conference on this subject (Ref. 1). All of the techniques presented in this conference for application to transonic shock induced separated flow are based on integral boundary layer procedures in which it is generally necessary to make several assumptions in order to close the system of equations. For example in these techniques semi-empirical relationships between the skin friction and momentum thickness or shape factor are used which have been specifically developed for "airfoil" type flows and thus may not be applicable to a wide range of flow conditions. The focus of the present research program is on the use of a finite difference inverse boundary layer procedure, embodied in a viscous-inviscid iteration procedure, which is free of this type of semi-empirical assumptions. It should be recalled however that for a finite difference solution of turbulent flows it is necessary to relate the Reynolds stress to the mean flow at each point across the boundary layer so as to close the system of equations. At the present time an adequate turbulence model for strongly interacting flows is yet to be developed. The present prediction technique offers an efficient procedure by which various turbulence models could be tested since this method provides a detailed resolution of the boundary layer flow and requires much less computer time than a numerical solution of the Navier-Stokes equations, where for example, turbulence model studies have been conducted for separated flows (Ref. 2).

The overall objective of the present contract is to demonstrate that a viscous-inviscid interaction procedure, previously developed for subsonic flows (Ref. 3), is applicable to the problem of transonic shock induced separated flow. In this interim technical report a brief description is presented of the overall technique and comparisons are made with the axisymmetric experimental data of Bachalo and Johnson (Ref. 4). Various numerical tests which have been performed are also discussed. These calculations are aided by the use of the new Werle-Verdon (Ref. 5) shear layer coordinate system which is aligned with an estimated position of the shear layer in the large separated region.

ANALYSIS

Shear Layer Coordinate System

The boundary layer equations are usually written in a body oriented coordinate system in which it is assumed that the pressure gradient normal to the surface is zero and the dominant viscous shear force is parallel to the surface. When flow separation occurs, the separated boundary layer follows a path which may differ significantly from the actual body shape. This difference becomes significant when the separated flow region is large as is depicted schematically in Fig. 1. In a similar flow problem, the viscous separated flow over a blunt trailing edge of an airfoil, Werle-Verdon (Ref. 5) proposed that a shear layer coordinate system be used which would eliminate artificial inviscid stagnation points thereby simplifying the overall interaction analysis. This coordinate system is chosen so as to align the viscous calculation with an estimated position of the separated shear layer as shown in Fig. 1. The boundary layer approximations are then made with respect to this coordinate system, which despite its estimated position, is preferable to the usual surface oriented coordinates for the separated flow over a body shape with a slope discontinuity such as that shown in Fig. 1. The inviscid flow is solved over the assumed position of the shear layer which is formed by adding the thickness t to the original body coordinate as shown in Fig. 1. This modified surface forms an estimate to the displacement surface which then is corrected in the viscous-inviscid iteration procedure by imposing an injection velocity which is normal to the shear layer coordinate and proportional to the difference in the actual and estimated displacement surfaces. Thus it is seen that with the use of this shear layer coordinate system the injection velocity is now significantly reduced as it is only used to represent the error in the assumed displacement thickness. In fact if the shear layer coordinate system were chosen to lay precisely on the displacement surface iteration would not be needed to determine the flow field. A study has been initiated to deduce the sensitivity of the final results to the choice of the shear layer coordinate and results obtained thus far will be discussed in this report.

Inverse Boundary Layer Procedure

The viscous solution technique used in the present investigation is the inverse boundary layer procedure presented by Carter (Ref. 3) for compressible laminar or turbulent flows. Catherall and Mangler (Ref. 6) were the first to show that the classical separation singularity can be eliminated in a boundary layer calculation by solving the equations inversely in which the displacement thickness is prescribed and the pressure distribution is deduced from the resulting solution. Since their pioneering paper there have been a number of

studies in which various inverse boundary layer techniques have been developed. The procedure used in the present report is a technique which has evolved from earlier work (Refs. 7 and 8) into a general boundary layer solution technique which can be solved in either the direct or inverse mode and is no more complicated than conventional finite difference techniques for the boundary layer equations.

In the present work the boundary layer equations are written in terms of the shear layer coordinate system discussed in the previous section. In this coordinate system the usual surface boundary conditions are imposed at $y = -t$. Werle and Verdon (Ref. 5) showed that it is convenient to transform the boundary layer equations by the Prandtl transposition theorem such that the classical form of these equations is retained with the same surface boundary conditions now imposed at $N = 0$ where $N = y + t$.

The development of the inverse formulation begins by transforming the equations, expressed in primitive variables, by the following transformation of the independent variables:

$$\xi = \int_0^s \rho_0 \mu_0 u_0 r_0^2 ds \quad \eta = \frac{1}{8\pi} \int_0^N \frac{\rho}{\rho_0} \frac{r}{r_0} dN \quad (1)$$

which is quite similar to the Levy-Lees transformation as modified by the inclusion of the transverse curvature terms as shown by Probstein and Elliot (Ref. 9). It is helpful to scale the normal coordinate by the displacement thickness in strongly interacting flows since this step insures that the boundary layer thickness is approximately constant in the transformed coordinate. A further improvement on this scaling would be to incorporate the adaptive grid technique recently presented by Carter, Edwards and Werle (Ref. 10). The continuity equation is eliminated by introducing the stream function

$$\rho u_r = \frac{\partial \psi}{\partial N} \quad \rho v_r = -\frac{\partial \psi}{\partial s} \quad (2)$$

The value of the stream function at the boundary layer edge is written in terms of the displacement thickness

$$\psi \rightarrow \rho_0 u_0 r_0 \left(\int_0^N \frac{r}{r_0} dN - \delta^+ \right) \quad \text{as} \quad N \rightarrow \infty \quad (3)$$

which with the definitions

$$m = \rho_0 u_0 \delta^* r_0 \quad h = \int_0^\infty \left(\frac{\rho_0}{\rho} - 1 \right) d\eta \quad (4)$$

can be written as

$$\psi \rightarrow m(\eta - 1 + h) \quad \text{as} \quad \eta \rightarrow \infty \quad (5)$$

A perturbation stream function is defined as

$$\tilde{f} = \frac{1}{\sqrt{2\xi}} [\psi - Fm(\eta - 1 + h)] \quad (6)$$

such that $\tilde{f} \rightarrow 0$ as $\eta \rightarrow 0$ for a prescribed m . Note that in the compressible inverse formulation the perturbation mass flow m is prescribed and not just the displacement thickness.

If the compressible, turbulent boundary-layer equations are transformed with Eq. (1) and the perturbation stream function defined in Eq. (6) is introduced into these equations then the following governing equations result:

$$\frac{\partial \tilde{f}}{\partial \eta} = \frac{m}{\sqrt{2\xi}} (1 - \eta - h) \frac{\partial F}{\partial \eta} \quad (7)$$

$$m^2 F \frac{\partial F}{\partial \xi} - m \frac{\partial}{\partial \xi} \left[\sqrt{2\xi} \tilde{f} + mF(\eta - 1 + h) \right] \frac{\partial F}{\partial \eta} = m^2 \beta (g - F^2) + \frac{\partial}{\partial \eta} \left[(1 + \frac{\epsilon}{\mu}) \ell \frac{\partial F}{\partial \eta} \right] \quad (8)$$

$$m^2 F \frac{\partial g}{\partial \xi} - m \frac{\partial}{\partial \xi} \left[\sqrt{2\xi} \tilde{f} + mF(\eta - 1 + h) \right] \frac{\partial g}{\partial \eta} = \\ \frac{1}{Pr} \frac{\partial}{\partial \eta} \left[\ell \left(1 + \frac{\epsilon}{\mu} \frac{Pr}{Pr_t} \right) \frac{\partial g}{\partial \eta} \right] + \frac{(\gamma - 1) M_0^2}{1 + \frac{\gamma - 1}{2} M_0^2} \frac{\partial}{\partial \eta} \left[\ell \left(1 - \frac{1}{Pr} \right) F \frac{\partial F}{\partial \eta} \right] \quad (9)$$

where

$$F = \frac{U}{U_e} \quad g = \frac{H}{H_e} \quad \beta = \frac{1}{M_e} \frac{dM_e}{d\xi} \quad \lambda = \frac{\rho\mu}{\rho_e\mu_e} \left(\frac{r}{r_0}\right)^2 \quad (10)$$

In these equations ϵ is the eddy viscosity coefficient which relates the Reynolds shear stress term to the normal gradient of the mean streamwise velocity component. In the present investigation the algebraic turbulence model of Cebeci and Smith (Ref. 11) has been used.

Equations (8) - (10) are solved for F , g , f and λ for a prescribed streamwise distribution of m subject to the following boundary conditions:

$$\left. \begin{array}{l} \eta=0 \quad F=\tilde{f}=0 \quad g=g_w \quad \text{or} \quad \left. \frac{\partial g}{\partial \eta} \right|_{w_0} \quad \text{specified} \\ \eta \rightarrow \infty \quad F=g \rightarrow 1 \quad \text{and} \quad \tilde{f} \rightarrow 0 \end{array} \right\} \quad (11)$$

These equations can also be solved in the direct mode with prescribed and the outer boundary condition $\tilde{f} = 0$ eliminated. In this case if m is set equal to $\sqrt{2\xi}$ then the usual Levy Lees formulation is deduced with the only difference being that the normal component of velocity has been reexpressed in terms of the stream function. The numerical solution of these equations for both the direct and inverse mode is an implicit finite difference technique which is first order accurate in the stream direction and second order accurate in the normal direction. In the inverse case the unknown pressure gradient parameter is deduced simultaneously with the remainder of the solution. The details of the numerical scheme are presented in Ref. 12.

Inviscid Analysis

The inviscid technique used in the present study is the transonic full potential analysis developed by South and Jameson (Ref. 13) with the computer program (RAXBOD) documented by Keller and South (Ref. 14). In this analysis a successive line over-relaxation procedure is applied to the finite difference form of the full potential equation for the inviscid flow over axisymmetric bodies in free air. For bodies with a sting this program uses a body-normal coordinate on the forebody up to the first horizontal tangent and a sheared cylindrical coordinate system aft of that point. In the present calculations the axisymmetric configuration (Ref. 4) which was analyzed has an open nose which required that modifications be made to the code to permit treatment of this particular shape. A stretching is applied to both the normal and tangential coordinates such that the infinite physical space is mapped to a finite computational space.

Viscous-Inviscid Iteration

The present analysis is based on a viscous-inviscid iteration technique which was previously demonstrated for subsonic flows (Ref. 3), and is outlined in Fig. 2. This procedure, which has been referred to as a semi-direct technique by LeBalleur (Ref. 15), combines an inverse boundary layer technique with a direct inviscid analysis via the update procedure shown in Fig. 2. The advantage of the semi-direct method is that it permits an inverse boundary-layer procedure, which is applicable to separated flow, to be combined with an existing inviscid analysis in which only a slight modification is required to include viscous displacement body effects. Another advantage of the semi-direct method is that in the boundary layer solution the unknown pressure gradient is deduced and then integrated to determine the pressure distribution. This integration provides a natural smoothing process in the solution and is probably the reason that no smoothing is required in the present viscous-inviscid iteration technique. In contrast most applications of the usual Prandtl iteration cycle for weakly interacting flows require the use of numerical smoothing and significant underrelaxation. In the present calculations the relaxation factor was varied from .75 to 1.0.

In the present technique the displacement thickness (or more precisely, $m = \rho_e u_e \delta^* r_0$) is prescribed for both the viscous and inviscid flows. Injection is used in the inviscid flow to represent the viscous effects in which the injection velocity is given by:

$$v_n = \frac{1}{\rho_e r_0} \left[\frac{dm}{ds} - \frac{d}{ds} (\rho_e u_e r_0) \right] \quad (12)$$

where t is the distance from the shear layer coordinate line to the surface measured perpendicularly to the shear layer coordinate line. After the viscous and inviscid flows are solved for a prescribed displacement thickness, a new displacement thickness distribution is determined from the mismatch predicted in the viscous and inviscid tangential velocities, u_e . The procedure then continues until convergence is obtained. This update procedure was originally an ad hoc assumption but further examination (Ref. 3) showed that it is somewhat analogous to the relationship between changes in u_e and m given by the von Karman momentum integral. The interaction procedure shown in Fig. 2 is general and has been used in a number of other studies (Refs. 5, 16, 17, 18) in which a variety of inverse boundary-layer and direct inviscid solvers have been employed.

RESULTS AND DISCUSSION

The prediction technique discussed briefly in the previous section has been applied to the axisymmetric circular arc bump of Bachalo and Johnson (Ref. 4) shown in Fig. 3 for which they have taken detailed experimental data at transonic flow conditions in the NASA-Ames 2 x 2 foot wind tunnel. Surface flow visualization studies revealed that the flow was two-dimensional throughout the interaction region including the vicinity of a relatively strong shock wave. A small fillet was placed at the leading edge of the circular arc bump so as to prevent separation in this region. It was deduced in the experiment and the present interaction calculations that the flow remain attached in this region. Bachalo and Johnson also stated that their measurements are free of tunnel blockage up to $M_\infty = 0.90$ for this model shape since the shock wave did not extend to the tunnel wall. Reduction in tunnel blockage is aided by the use of an axisymmetric model as compared to a two-dimensional shape since the shock wave strength decreases with the inverse square of the distance in the axisymmetric case and with the inverse of the distance for a plane two-dimensional configuration.

Upstream Boundary Layer Analysis

Since the flow disturbance caused by the presence of the circular arc bump did not extend all the way to leading edge of the front sting, the interaction between the viscous and inviscid flow, which is dominant near the bump-rear sting juncture point, was assumed to be negligible from the leading edge to the start of the pressure rise as the flow approached the bump. The initial boundary layer profile was determined by solving the viscous equations in the direct mode from the leading edge to a point downstream subject to the inviscid pressure distribution determined from the RAXBOD code. Figure 4 shows good agreement between the skin friction distribution determined from the present direct calculation and that obtained from the UTRC boundary layer code which is called ABLE; Analysis of Boundary Layer Equations (Ref. 19). Both codes were subjected to the same pressure distribution. Transition from laminar to turbulent flow was assumed to occur at $x/c = -2.88$, where x is measured from the start of the circular arc bump as shown in Fig. 3. It is seen in Fig. 4 that the skin friction decreases rapidly as the bump is approached; hence it was decided to set the initial boundary layer profile at $x/c = -0.54$ (denoted by an arrow in Fig. 4) for the downstream interaction analysis. Figure 5 shows a favorable comparison between these two direct boundary layer solutions for the velocity profiles at $x/c = -.125$ and $.125$ and the experimental data of Bachalo, Modaress, and Johnson (Ref. 20).

Comparison with Experiment

Figure 6 shows the two shear layer coordinate lines which were used in the present calculations. Both are cubic fillets which connect the circular arc bump to the downstream sting. The first one was chosen arbitrarily and the second was prescribed so as to approximately match the experimental displacement surface which is also shown in Fig. 6. Also shown are the shock wave, and the separation and reattachment positions deduced experimentally by Bachalo and Johnson (Ref. 4). It is observed from Fig. 6 that despite the large separated flow region the body radius is sufficiently large in comparison to the displacement thickness that traverse curvature effects could be considered negligible and thus the radius r was set equal to the body radius r_0 in the governing equations for the viscous flow.

Interacted boundary-layer results are shown in Fig. 7 for the pressure distribution along with that measured experimentally by Bachalo and Johnson (Ref. 4) and the Navier-Stokes solution reported by Johnson, Horstman, and Bachalo (Ref. 21). The present results were obtained using coordinate line number one and the upstream boundary layer profiles at $x/c = -.54$ which were previously discussed. Comparison of the inviscid solution, also shown in Fig. 7, with the interacted boundary-layer solution shows that inclusion of the viscous effects moves the shock upstream and in general improves the overall agreement with the experimental data. Although the interacted boundary layer solution predicts the shock position reasonably well, the pressure in the body sting juncture region is significantly overpredicted. This result is consistent with the underprediction of the displacement thickness in this region as shown in Fig. 8. The extent of the separated flow is also underpredicted. The displacement thickness distribution deduced from the solution of the Navier-Stokes equations is also shown in Fig. 8. Comparison of Figs. 7 and 8 shows that the best agreement in the Navier-Stokes solution with the pressure data occurs in the same streamwise region where the best agreement is obtained with the experimental displacement thickness. This observation suggests that the displacement body is the principal interaction mechanism between the viscous and inviscid flows.

The present interacted boundary layer solution represents the first time, to this author's knowledge, that an inverse finite-difference boundary layer procedure has been iteratively combined with an inviscid analysis to obtain converged results for transonic flow with shock waves. Inverse boundary layer calculations were also performed by Johnson et. al. (Ref. 21) for the skin-friction distribution deduced from their solution of the Navier-Stokes equations for this particular case. These calculations were not interacted with an inviscid analysis as was done in the present calculations. In addition,

Johnson et. al. (Ref. 21) obtained non-unique solutions with their inverse boundary layer technique. It is not clear as to the source of their difficulty but it seems preferable, as state previously (Ref. 22), to use the displacement thickness instead of the skin friction as the basis of the inverse boundary layer procedure because of the natural role it plays in the matching of the viscous and inviscid flows.

The present calculations were obtained with an inviscid mesh of 81 points in the streamwise direction and 41 in the normal direction. These points were spread nonuniformly along the surface with the largest concentration of points placed near the shock wave. In the present case the minimum inviscid step size in the stream direction is $\Delta x/c = .024$. For the inverse viscous solution, which was initiated at $x/c = -.54$, 100 points were placed along the surface and 100 points across the boundary layer. The streamwise mesh was varied with a geometric progression such that the minimum step size, $\Delta x/c = .019$, occurred at the circular arc-sting juncture. Figure 9 shows the iterative history of this particular calculation in which the root-mean-square of the displacement thickness changes per streamwise grid point has been plotted against the iteration counter. There was some concern that the solution was not sufficiently converged after 12 global iteration cycles, hence the calculation was continued for another 10 cycles. Since a "perfect" restart capability does not currently exist in this interaction code a small initial jump occurred in the calculation when it was resumed. As can be seen in Fig. 9 the calculation continues to converge when it is continued. Convergence is monitored in several other ways as well so as to insure that no iteration difficulties are encountered. These calculations were obtained with an underrelaxation factor of .75 on the displacement thickness between successive iterations. In addition, it should be noted that for each global iteration cycle a maximum of 25 streamwise relaxation cycles were used in the inviscid solver and a maximum of 10 iterations were used in the boundary layer solution at each streamwise station.

There are a number of sources of error that need to be examined in order to determine the cause of the discrepancy between the predicted and experimental results. For example, the overall flow model here is an approximation to that represented by the Navier-Stokes equations. In addition the sensitivity of the solution to the mesh size, the turbulence model, and the assumed shear layer coordinate surface must be examined. As an initial step in this error study the shear layer coordinate surface was modified to coordinate line number two so that it approximates the experimental displacement surface as shown in Fig. 6. The inviscid analysis was then applied to the flow over this surface to determine if the displacement body concept is valid for this separated flow. Comparison of the predicted and the measured pressures are shown in Fig. 10 and it is seen that the agreement is improved substantially over that shown in Fig. 7. The experimental displacement thickness was then input to the inverse

boundary layer procedure and the resulting pressure, expressed in terms of the velocity at the edge of the boundary layer, is significantly overpredicted in the body sting juncture region as shown in Fig. 11. Since the test with the inviscid flow seems to verify the overall displacement body concept, this latter mismatch indicates that the turbulence model in the boundary layer technique may be a source of error. In these calculations the algebraic eddy viscosity model of Cebeci and Smith (Ref. 11) has been used which is generally considered to be highly approximate for separated turbulent flows. As an additional check on possible sources of error in the present calculations, the viscous-inviscid iteration procedure was carried out with shear layer coordinate line number two to see if the final interacted results were sensitive to the choice of shear layer coordinates. As can be seen in Fig. 6 the assumed surface differs significantly in the corner region; nonetheless the final results were nearly identical thereby indicating the lack of sensitivity to the assumed coordinate line.

In order to test the sensitivity of the overall flow prediction to the turbulence model several calculations were made in which the constants in the Cebeci Smith model were altered. These changes were made so as to increase the relative dominance of the wake portion of the two layer eddy viscosity model since it is known that the wall layer (log layer) vanishes as the separation point is approached. One way that this change can be made is by decreasing the empirical constant determined by Clauser ($\alpha = .0168$) thereby moving the match point between the inner and outer layers closer to the wall thus making the boundary layer more "wake like". The computed results obtained by reducing the Clauser constant from .0168 to .0084 resulted in significant improvement in the comparison with the experimental data as shown for the pressure in Fig. 12 and the displacement thickness in Fig. 13. Comparison of the interacted skin friction distributions is shown in Fig. 14 where it is seen that this modification has only a small influence on the skin friction upstream of the shock wave in the expanding part of the flow, but has a substantial effect from the shock wave downstream. Figure 15 shows a comparison of the computed velocity profiles and the experimental data at several locations for the different values of the Clauser constant. Again significant improvement in the agreement with the data (Ref. 21) is observed for the calculations made with the reduced wake constant. This change in the turbulence model is admittedly an ad hoc assumption; however, the Clauser constant was determined from equilibrium turbulent boundary layer flows and thus is probably not at all applicable to the highly nonequilibrium flow under study here. In fact it seems remarkable that such a simple change can improve the agreement with the experiment to this extent. Perhaps this simple test suggests that a generalized eddy viscosity model can be developed for separating flows, provided that the various streamwise regions can be modeled, as was recently done by Kim, et. al. (Ref. 23) from their experimental measurements, for the flow downstream of reattachment.

The present calculations were performed with the inviscid flow solved by the transonic potential flow analysis of South and Jameson (Ref. 13) which is a nonconservative analysis. This analysis is known to have a small but spurious mass source at the shock wave (Ref. 24) which generally results in the shock wave position being moved forward from that deduced in a conservative analysis. Figure 16 shows a comparison of the nonconservative solution obtained from the RAXBOD code with the conservative solution obtained by Green (Ref. 25) from the CONRAX code (conservative version of RAXBOD) for the inviscid flow over the circular arc bump configuration of Bachalo and Johnson. It is observed that the result obtained in the conservative analysis places the shock further aft and also gives a slightly different pressure distribution downstream of the sharp corner. In future work it is planned to incorporate the conservative inviscid analysis into the present interaction code and repeat the interaction analysis discussed in the present report.

CONCLUDING REMARKS

In the present study it has been demonstrated that a viscous-inviscid interaction approach, previously developed and demonstrated by the author for subsonic turbulent separated flows can be successfully applied to the problem of transonic shock induced separated flow. Converged solutions have been obtained and favorable comparisons with experimental data show that this method is capable of resolving the detailed features of this strongly interacting flow. In future work it is recommended that prior to the application of this technique to more complicated flows such as that over an airfoil further studies be conducted to determine the impact on the computed results of grid size both in the viscous and inviscid analyses, Mach number, and the conservative form of the inviscid potential flow equation. The present finite difference boundary layer technique is free of the semi-empirical assumptions used in the various integral techniques now applied to separated flows, but nonetheless requires a turbulence model to relate the Reynolds stress terms to the mean flow quantities. An adequate turbulence model does not currently exist for the type of flow fields analyzed in the present contract; however, the present method provides an excellent test bed by which various turbulence models could be explored in order to determine their applicability to strongly interacting viscous-inviscid flows.

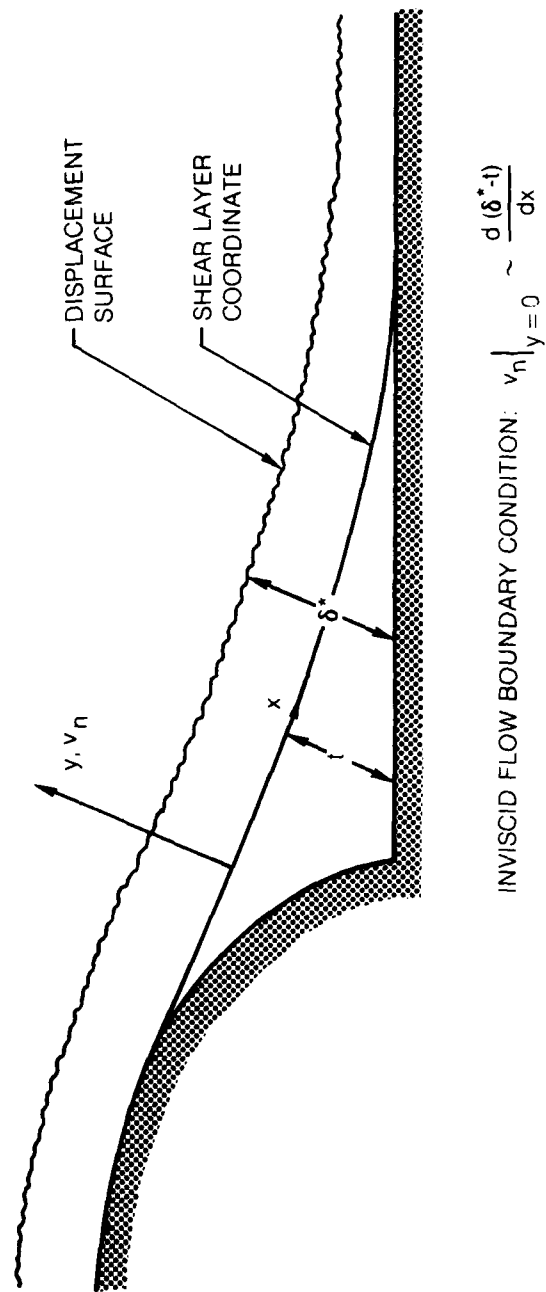
REFERENCES

1. Computation of Viscous-Inviscid Interactions, AGARD Conference Preprint No. 291, September 29 - October 1, 1980.
2. Viegas, J. R. and C. C. Horstman: Comparison of Multiequation Turbulence Models for Several Shock Boundary-Layer Interaction Flows. AIAA Journal, Vol. 17, No. 8, August 1979.
3. Carter, J. E.: A New Boundary-Layer Inviscid Iteration Technique for Separated Flow. AIAA Paper No. 79-1450, AIAA 4th Computational Fluid Dynamics Conference, Williamsburg, VA, July 23-25, 1979.
4. Bachalo, W. D. and D. A. Johnson: An Investigation of Transonic Turbulent Boundary Layer Separation Generated on An Axisymmetric Flow Model. AIAA Paper No. 79-1479, July 1979.
5. Werle, M. J. and J. M. Verdon: Viscid Inviscid Interaction for Symmetric Trailing Edges. Naval Air Systems Command Contractd N00019-78-C-0604. January 1980.
6. Catherall, D. and K. W. Mangler: The Integration of the Two-Dimensional Laminar Boundary-Layer Equations Past the Point of Vanishing Skin Friction. J. Fluid Mech., Vol. 26, Pt. 1, September 1966.
7. Carter, J. E.: Solutions for Laminar Boundary Layers with Separation and Reattachment. AIAA Paper No. 74-583, June 1974.
8. Carter, J. E. and S. F. Wornom: Solutions for Incompressible Separated Boundary Layers Including Viscous-Inviscid Interaction. Aerodynamic Analyses Requiring Advanced Computers, Part I. NASA SP-347, pp. 125-150.
9. Probstein, R. F. and D. Elliott: The Transversed Curvature Effect in Compressible Axiall Symmetric Laminar Boundary-Layer Flow. Journal of Aeronautical Sciences, March 1956, pp. 208-224.
10. Carter, J. E., D. E. Edwards and M. J. Werle: A New Coordinate Transformation for Turbulent Boundary Layer Flows, presented at NASA-Langley Workshop on Grid Generation Techniques for Partial Differential equations, October 6-7, 1980.
11. Cebeci, T. and A. M. O. Smith: Analysis of Turbulent Boundary Layers, Academic Press, 1974.
12. Carter, J. E.: Inverse Boundary Layer Theory and Comparison with Experiment. NASA TP-1208, September 1978.

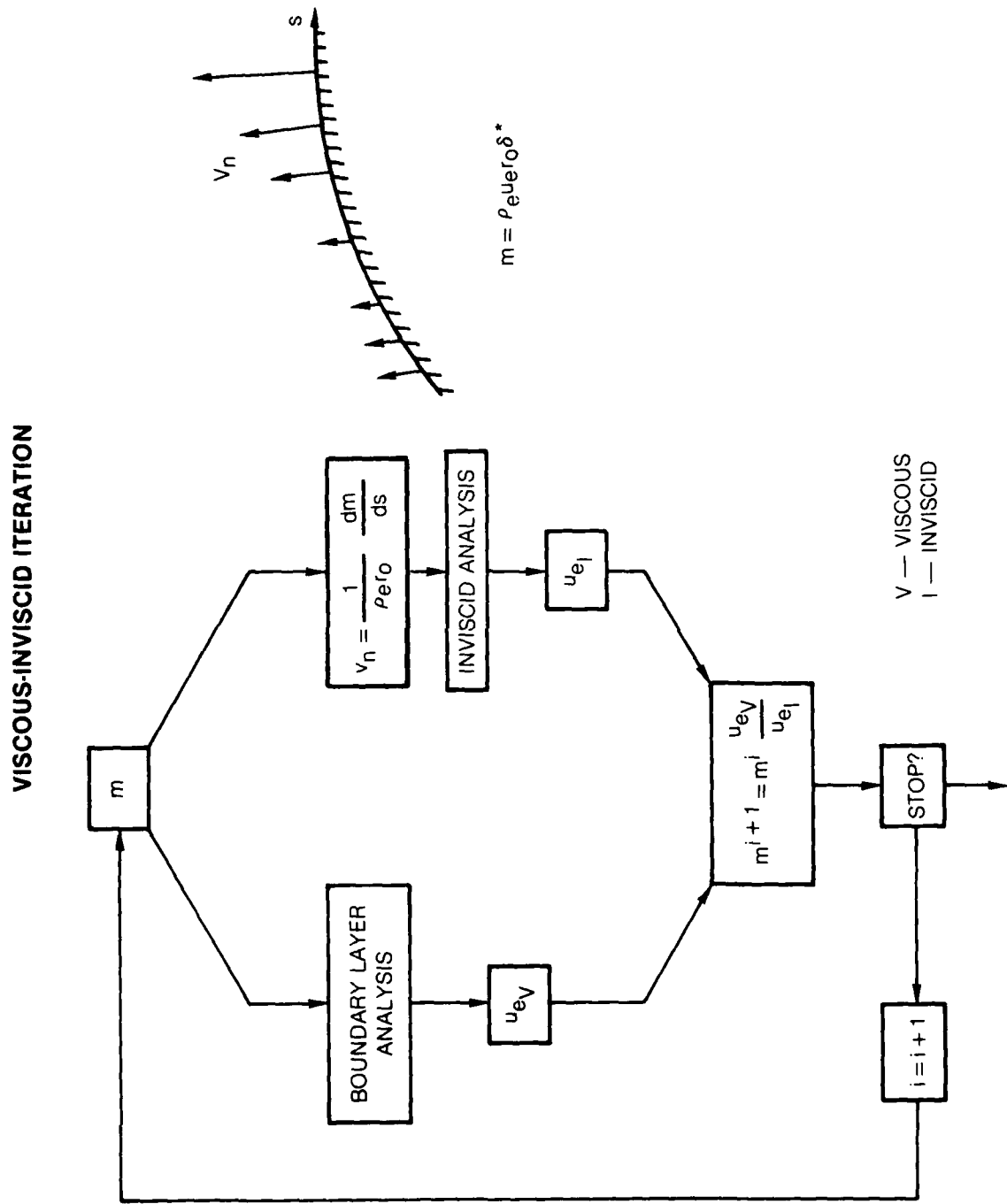
REFERENCES (Cont'd)

13. South, J. C., Jr. and A. Jameson: Relaxation Solutions for Inviscid Axisymmetric Transonic Flow Over Blunt or Pointed Bodies. AIAA Computational Fluid Dynamics Conference, Palm Springs, CA., pp. 8-17, July 1973.
14. Keller, J. D. and J. C. South, Jr.: RAXBOD: A Fortran Program for Inviscid Transonic Flow Over Axisymmetric Bodies. NASA TMX-72831, Feb. 1976.
15. LeBalleur, J. C.: Couplaged Visqueux - Non Visqueux: Methode Numerique et Applications Aux Ecoulements Bidimensionnels Transsoniques et Supereniques, La Recherche Aerospaile, No. 1978-2, p. 65-76.
16. Kuhn, G. D.: An Improved Interaction Method for Exhaust Nozzle Boattail Flows. AIAA Paper No. 80-0197, January 1980.
17. Whitfield, D. L., T. W. Swafford and J. J. Jacocks: Calculation of Turbulent Boundary Layers with Separation, Reattachment and Viscous-Inviscid Interaction. AIAA Paper No. 80-1439, July 1980.
18. Kwon, O. K. and R. H. Pletcher: Prediction of Incompressible Separated Boundary Layers Including Viscous-Inviscid Interaction. Presented at ASME Symposium on Turbulent Boundary Layers, June 1979.
19. Carter, J. E. and D. E. Edwards: Analysis of Compressible Laminar, Transitional and Turbulent Boundary Layer Equations, UTRC Report in Preparation, 1980.
20. Bachalo, W. D., D. Modarress and D. A. Johnson: Experiments on Transonic and Supersonic Turbulent Boundary Layer Separation. AIAA Paper No. 77-47, January 1977.
21. Johnson, D. A., C. C. Horstman and W. D. Bachalo: A Comprehensive Comparison Between Experiment and Prediction for a Transonic Turbulent Separated Flow. AIAA Paper No. 80-1407, July 1980.
22. Carter, J. E.: Inverse Solutions for Laminar Boundary-Layer Flows with Separation and Reattachment. NASA TR R-447, 1975.
23. Kim, J., S. J. Kline and J. P. Johnston: Investigation of a Reattaching Turbulent Shear Layer: Flow Over a Backward-Facing Step, Journal of Fluids.
24. Newman, P. A. and J. C. South, Jr.: Influence of Nonconservative Differencing on Transonic Streamline Shapes. AIAA J., Vol. 14, No. 8, August 1976, pp. 1148-1149.
25. Green, L. L.: NASA Langley Research Center, Private Communication, November 1980.

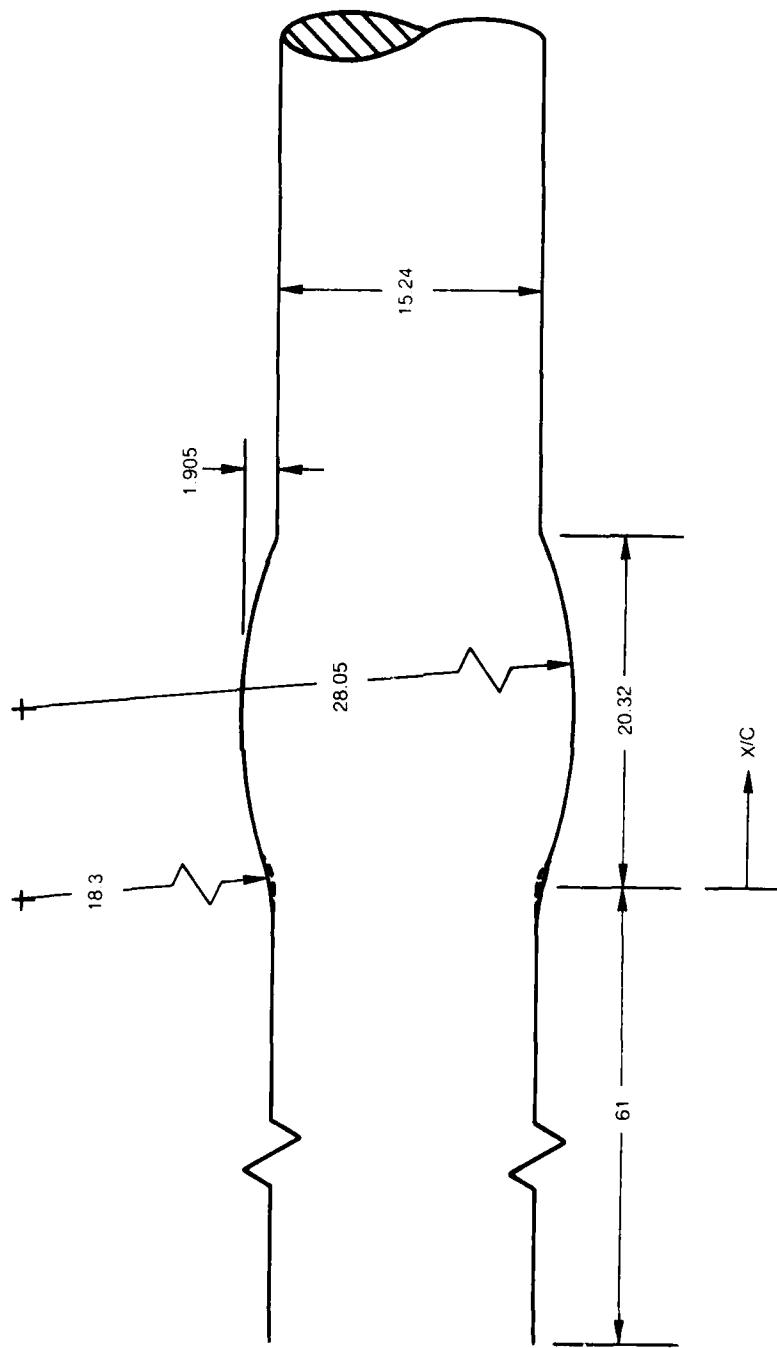
SHEAR LAYER COORDINATE SYSTEM



$$\text{INVISCID FLOW BOUNDARY CONDITION: } v_n \Big|_{y=0} \sim \frac{d(\delta^*)}{dx}$$



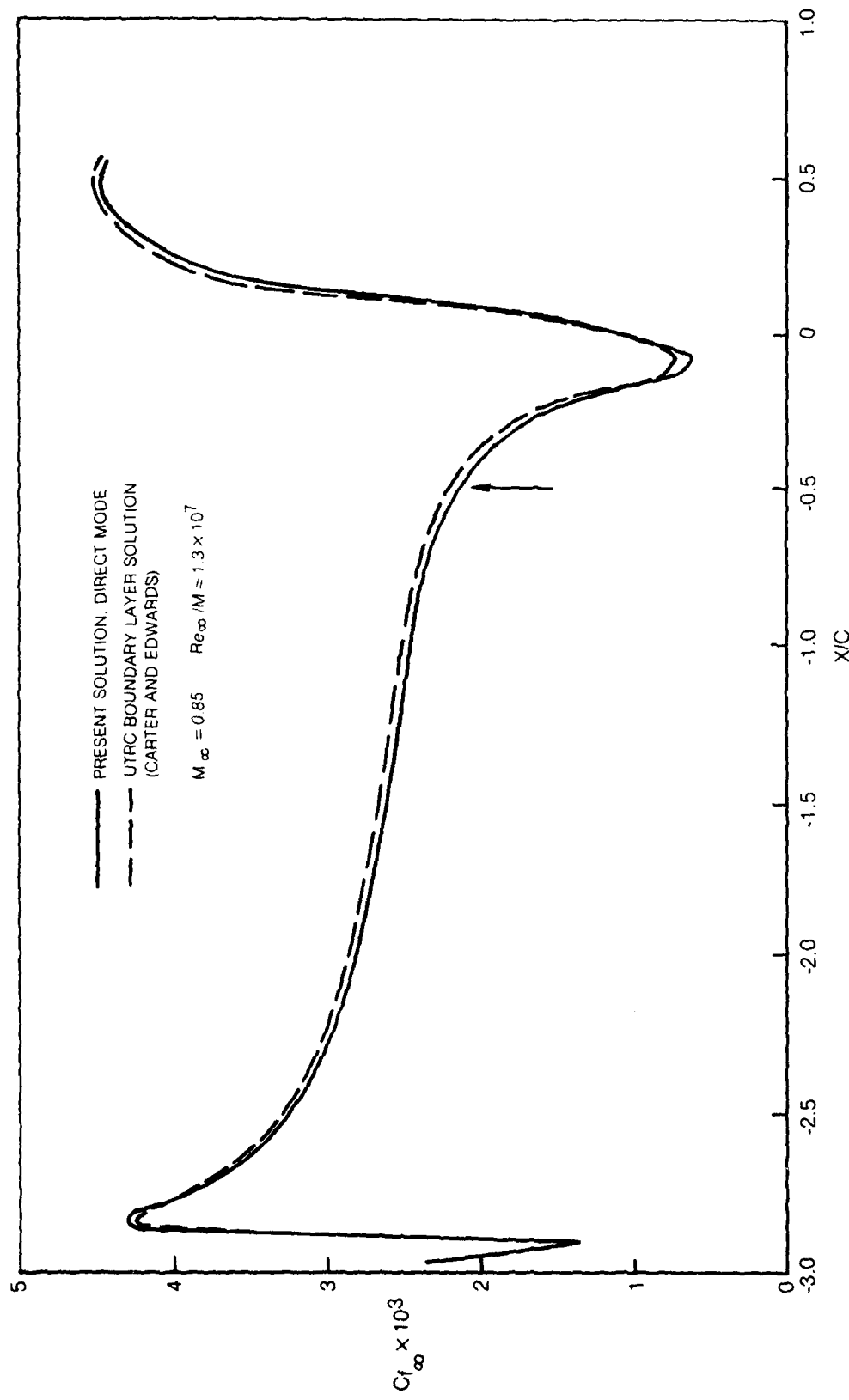
AXISYMMETRIC CIRCULAR ARC BUMP OF BACHALO AND JOHNSON



ALL DIMENSIONS ARE IN CENTIMETERS

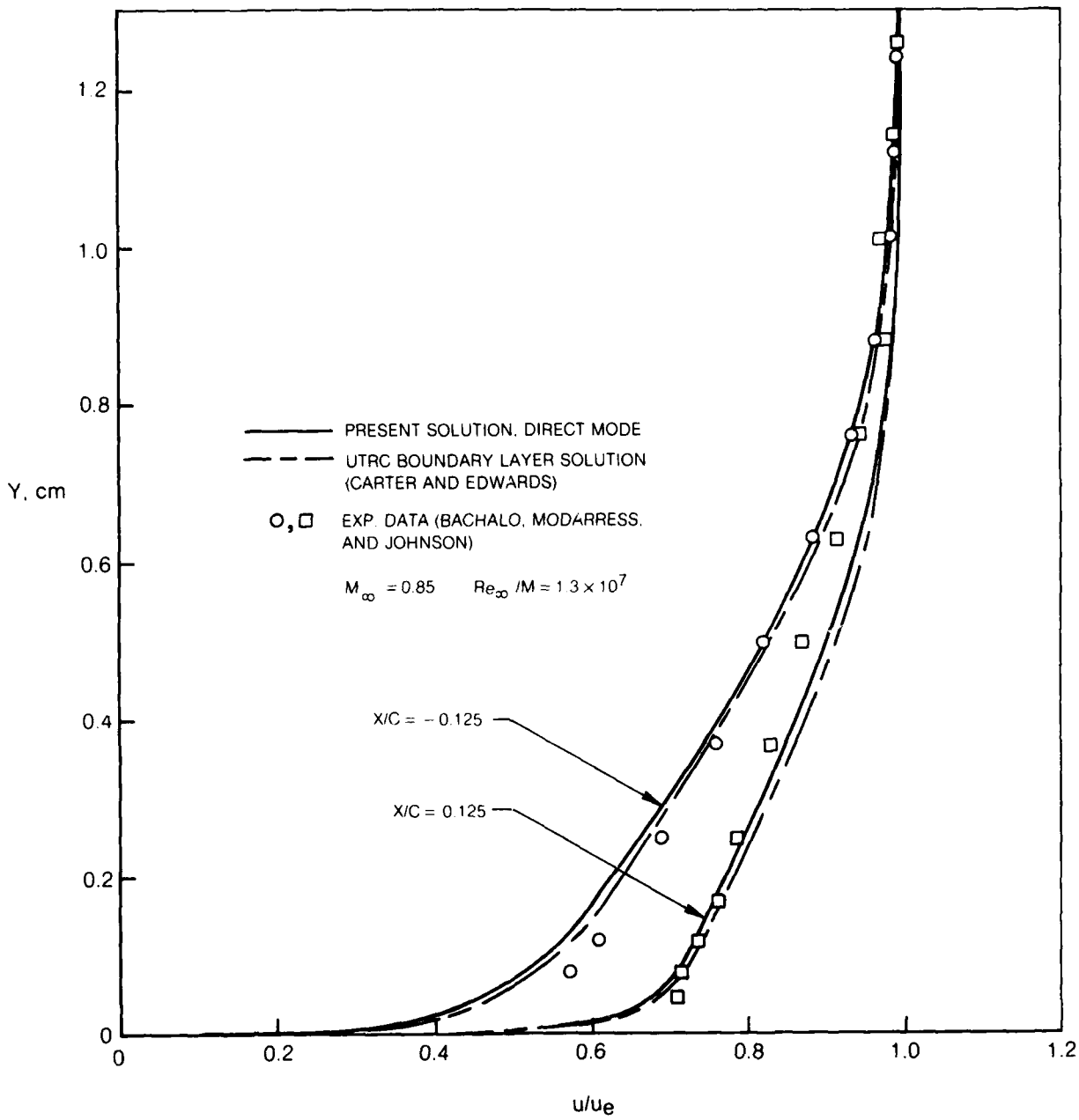
FIG. 4

SKIN FRICTION DISTRIBUTIONS UPSTREAM OF SHOCK WAVE

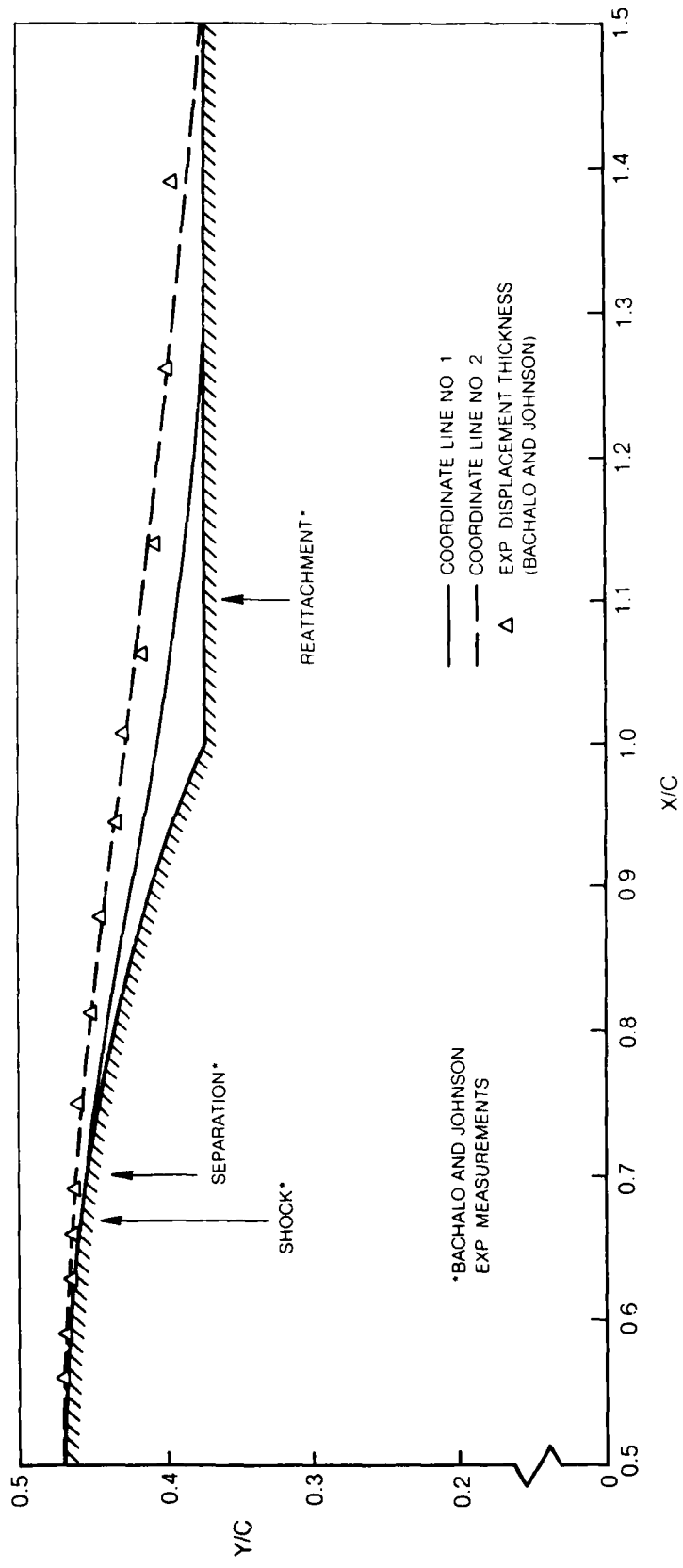


80-12-90-2

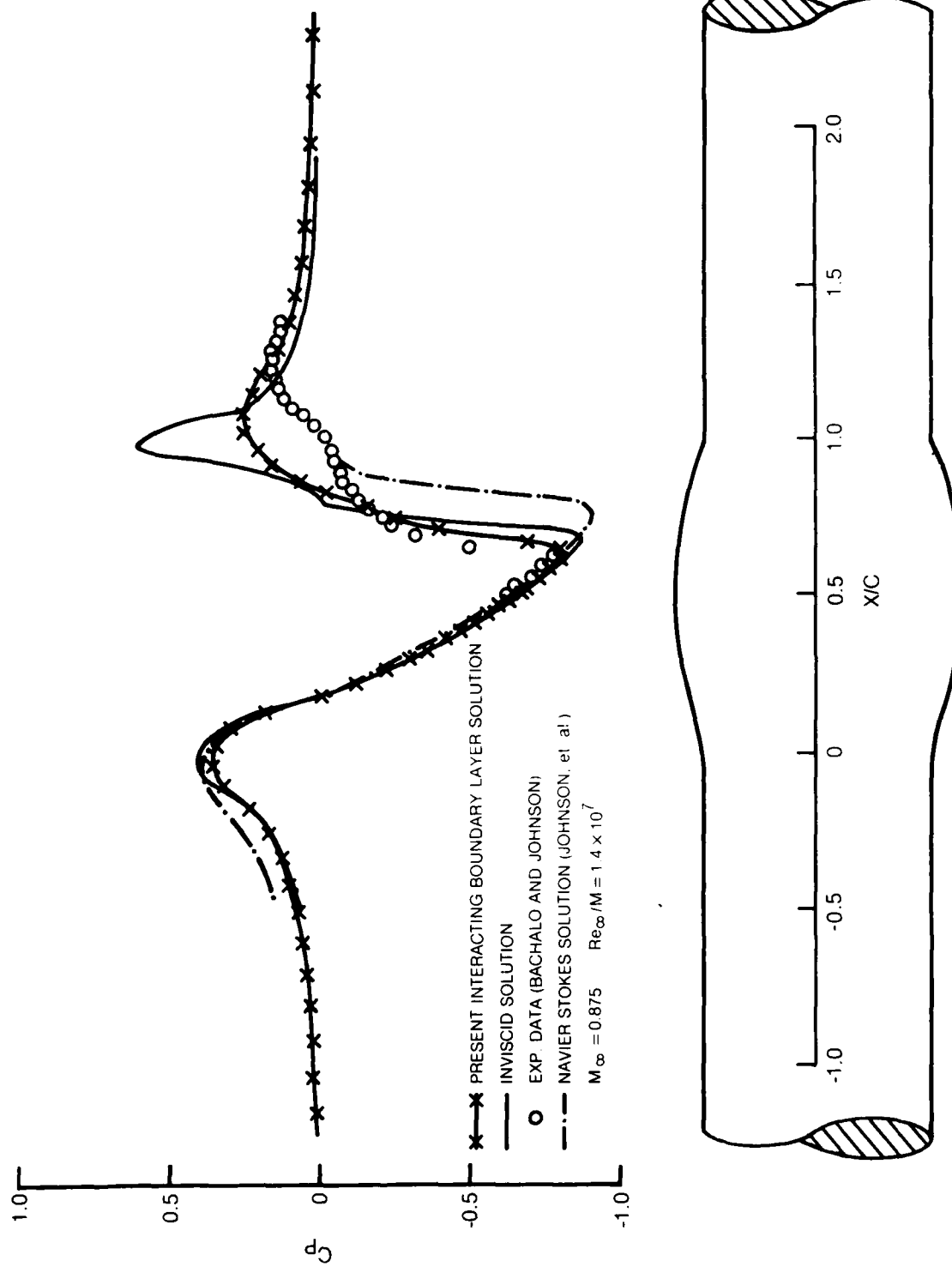
VELOCITY PROFILES UPSTREAM OF SHOCK WAVE



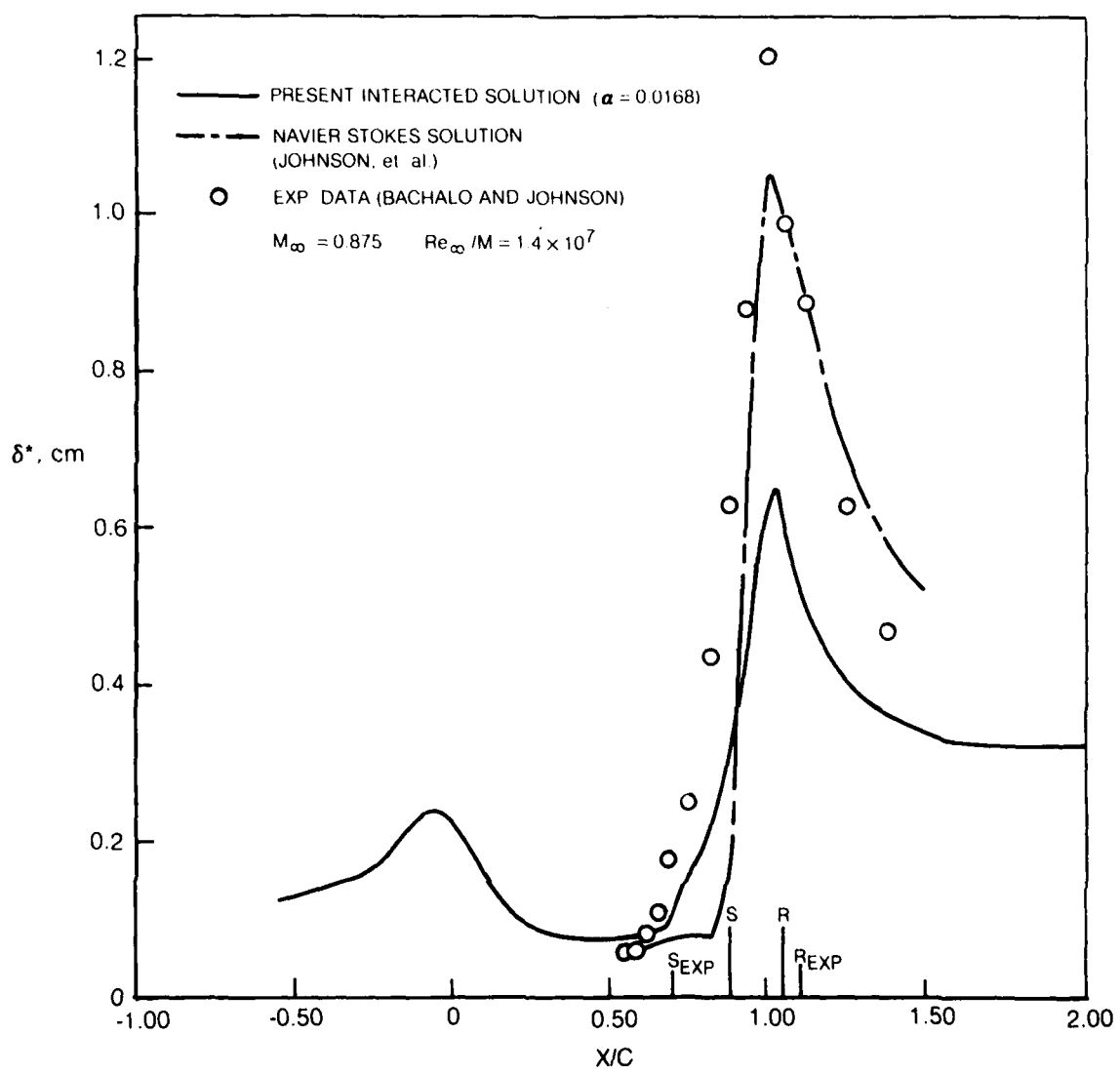
SHEAR LAYER COORDINATE LINES



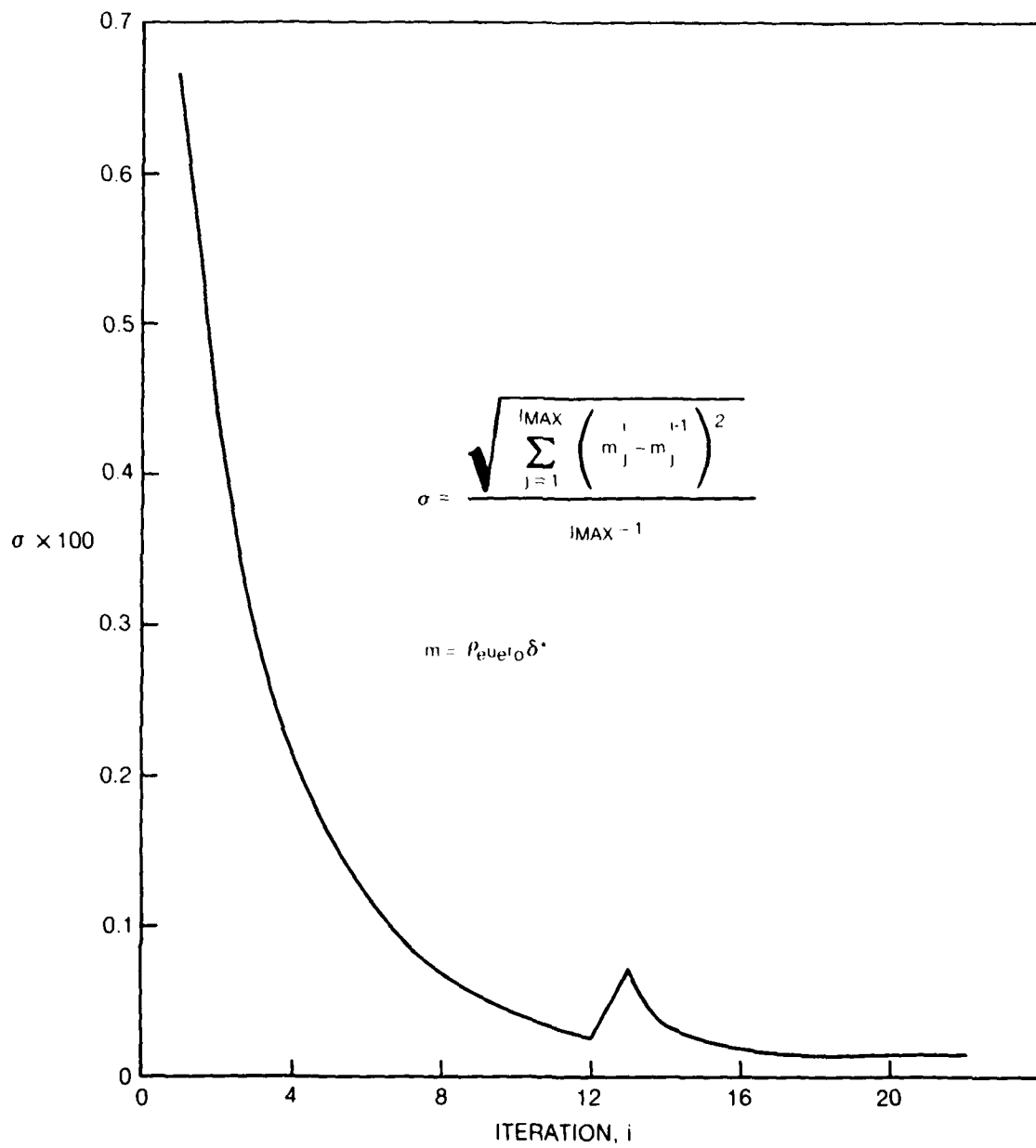
PRESSURE DISTRIBUTIONS AND BODY SHAPE

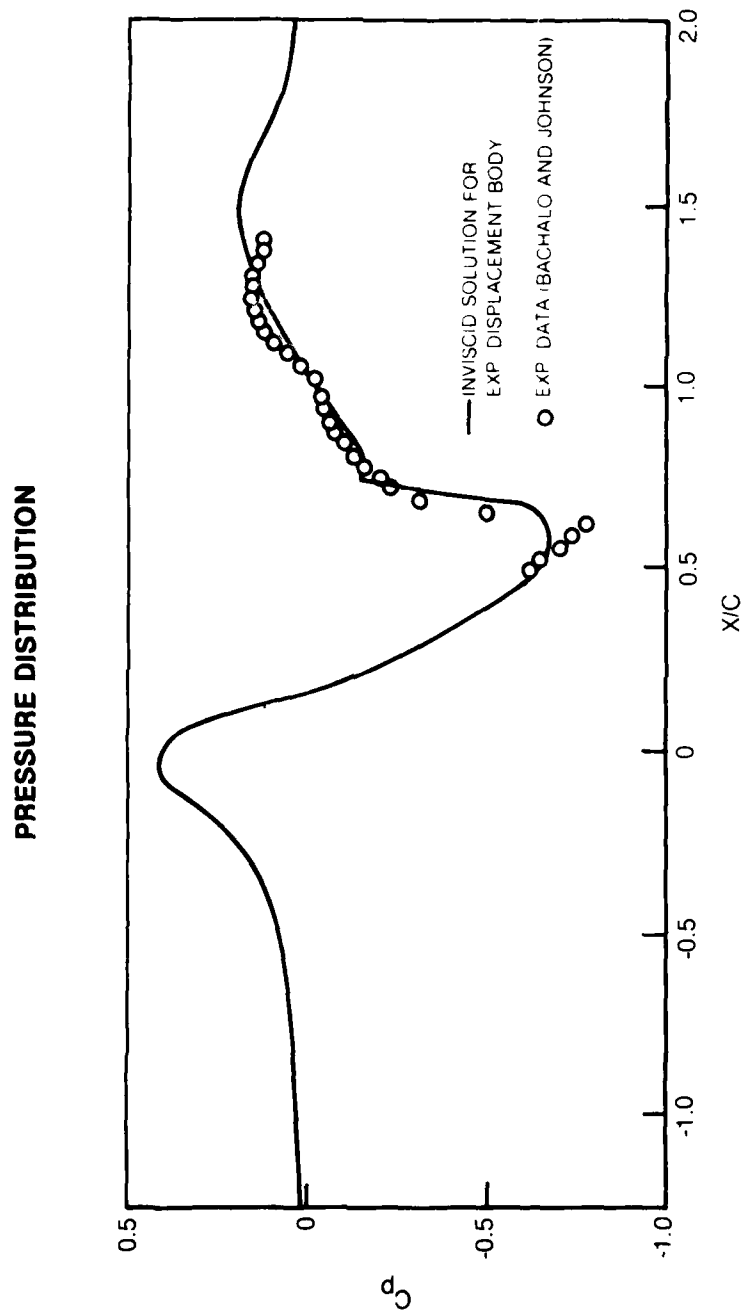


DISPLACEMENT THICKNESS DISTRIBUTIONS



ITERATIVE HISTORY





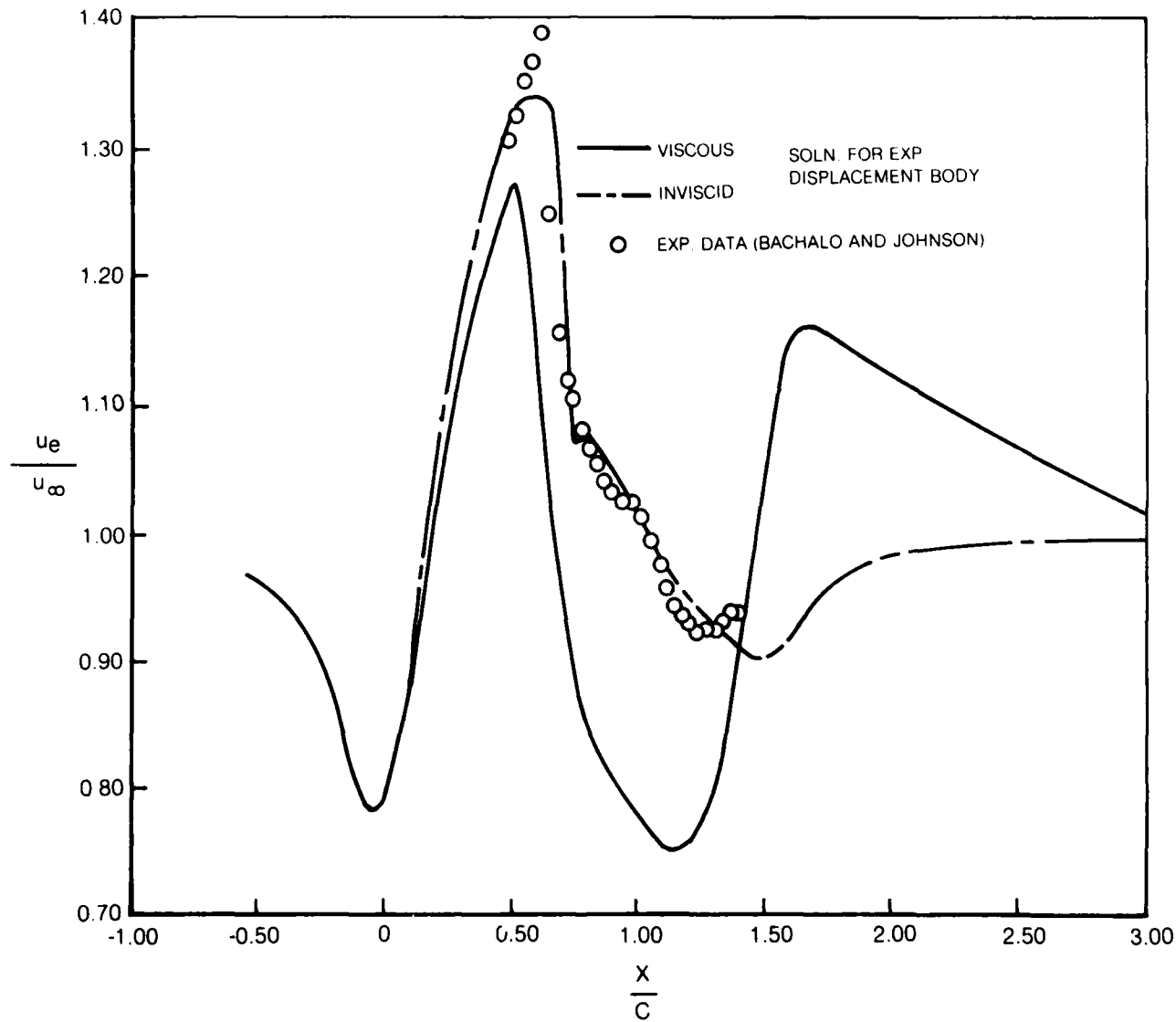
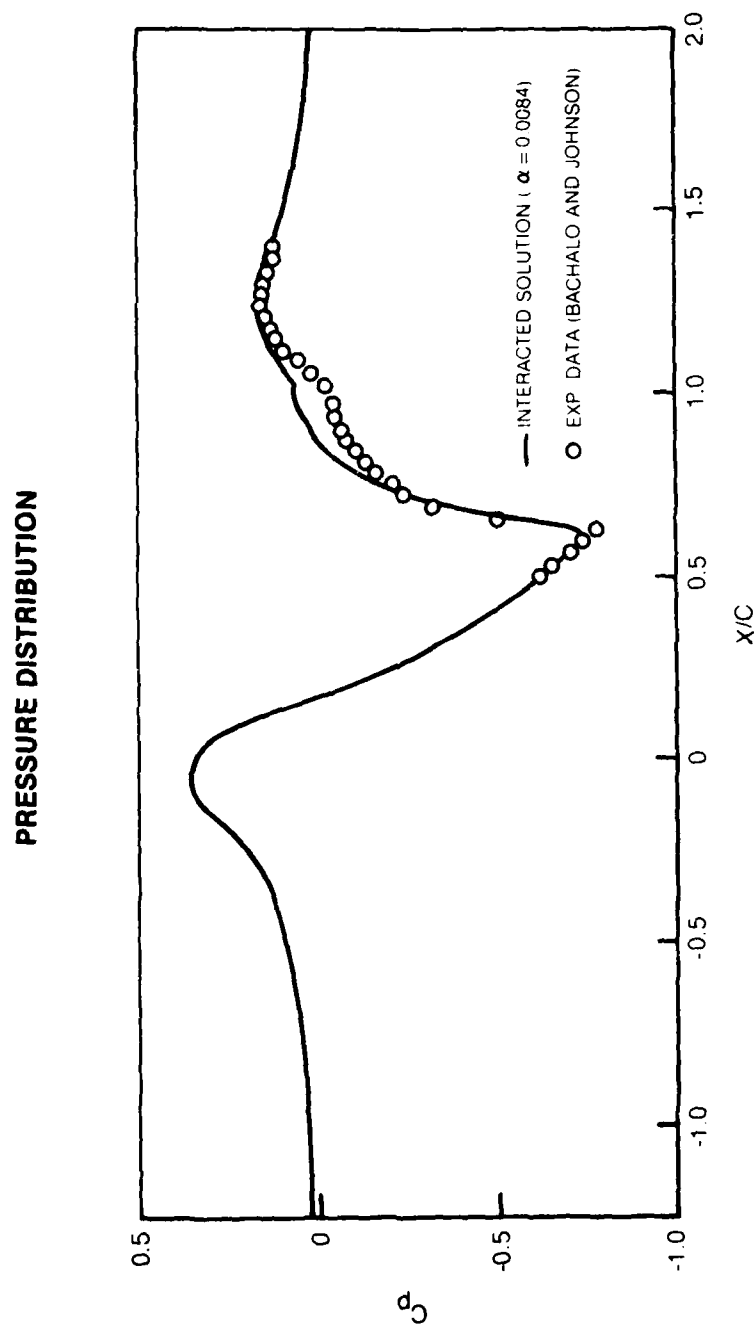
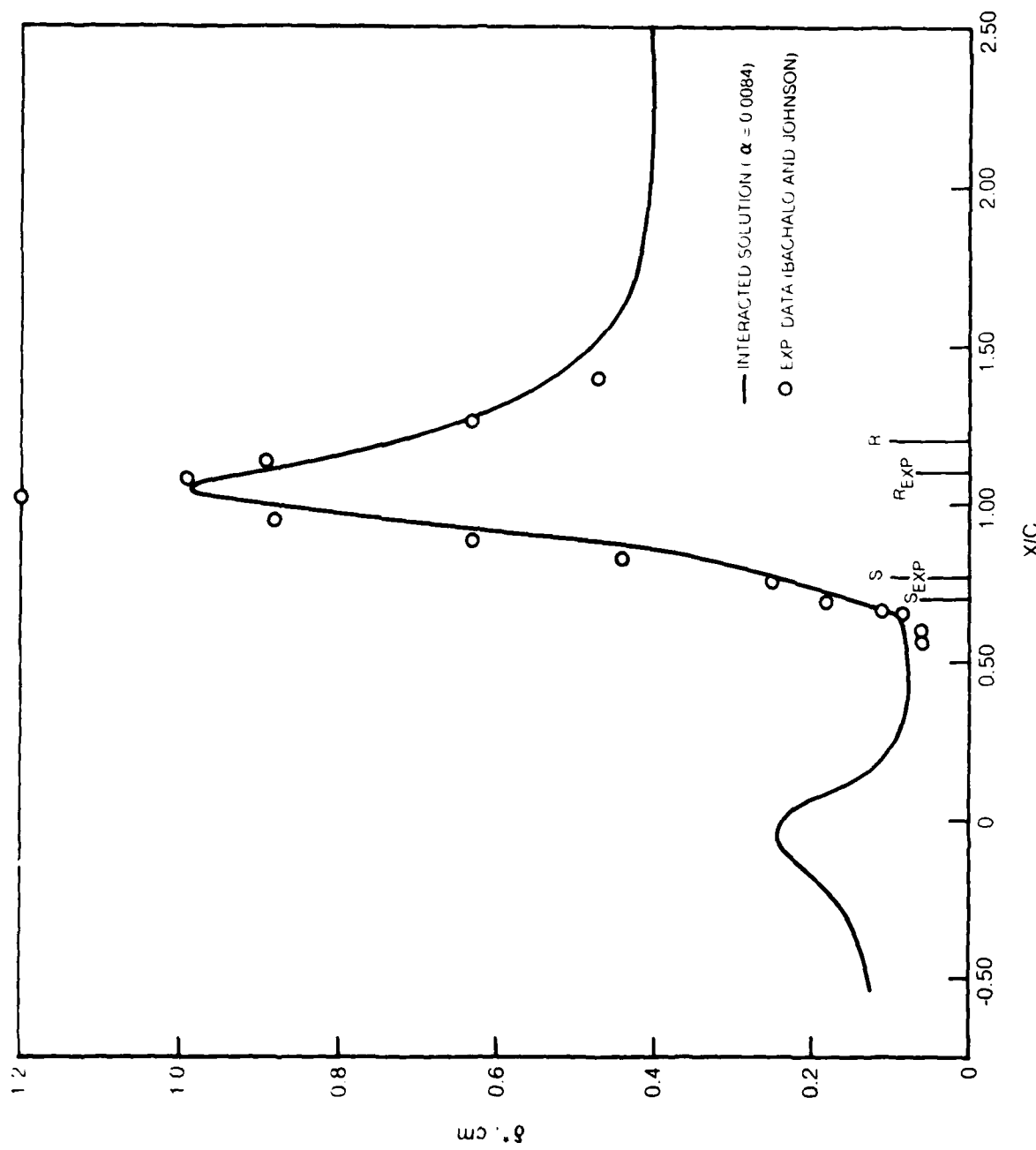
EDGE VELOCITY DISTRIBUTIONS

FIG. 12



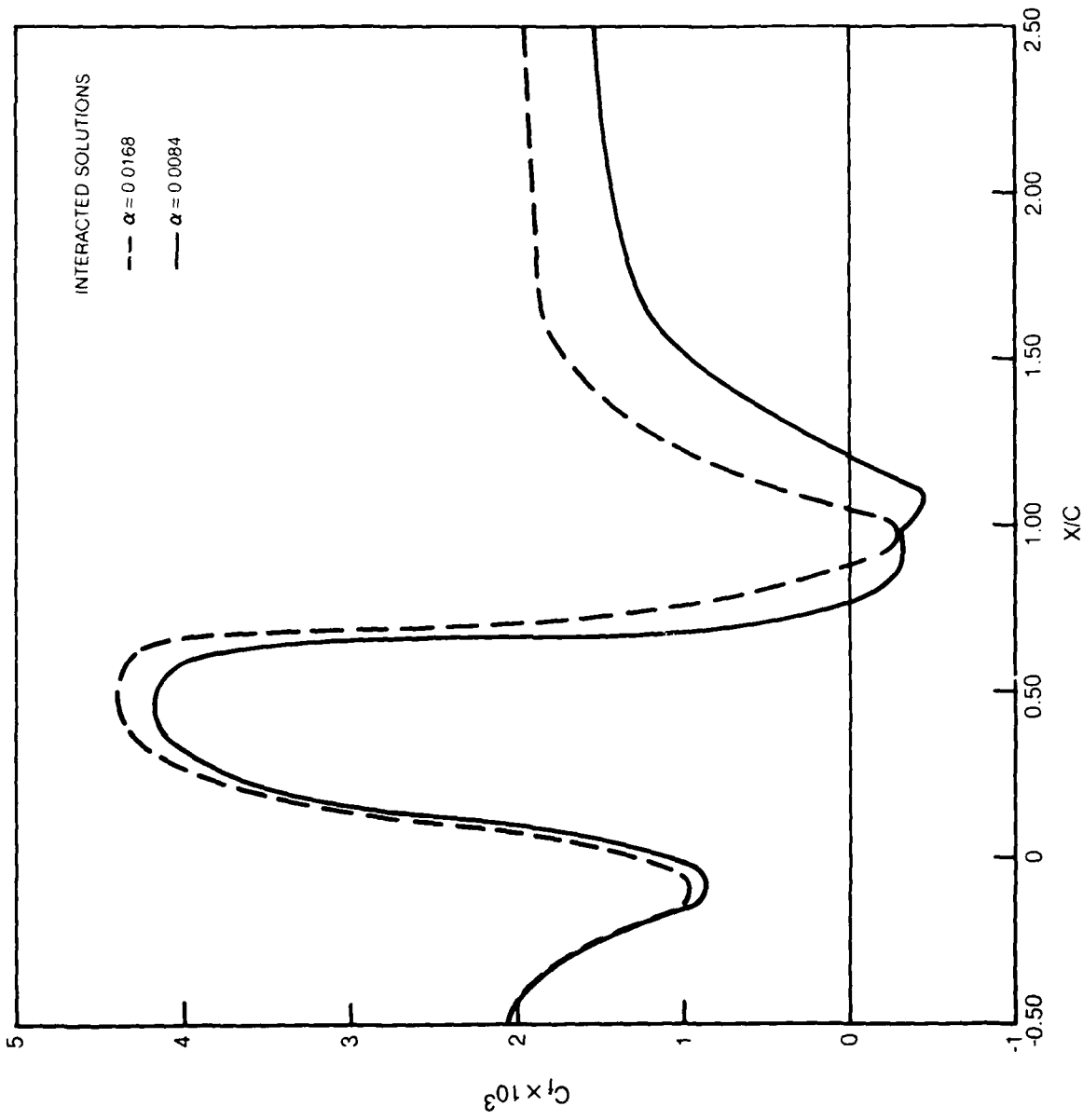
DISPLACEMENT THICKNESS DISTRIBUTION



R80-915213-4

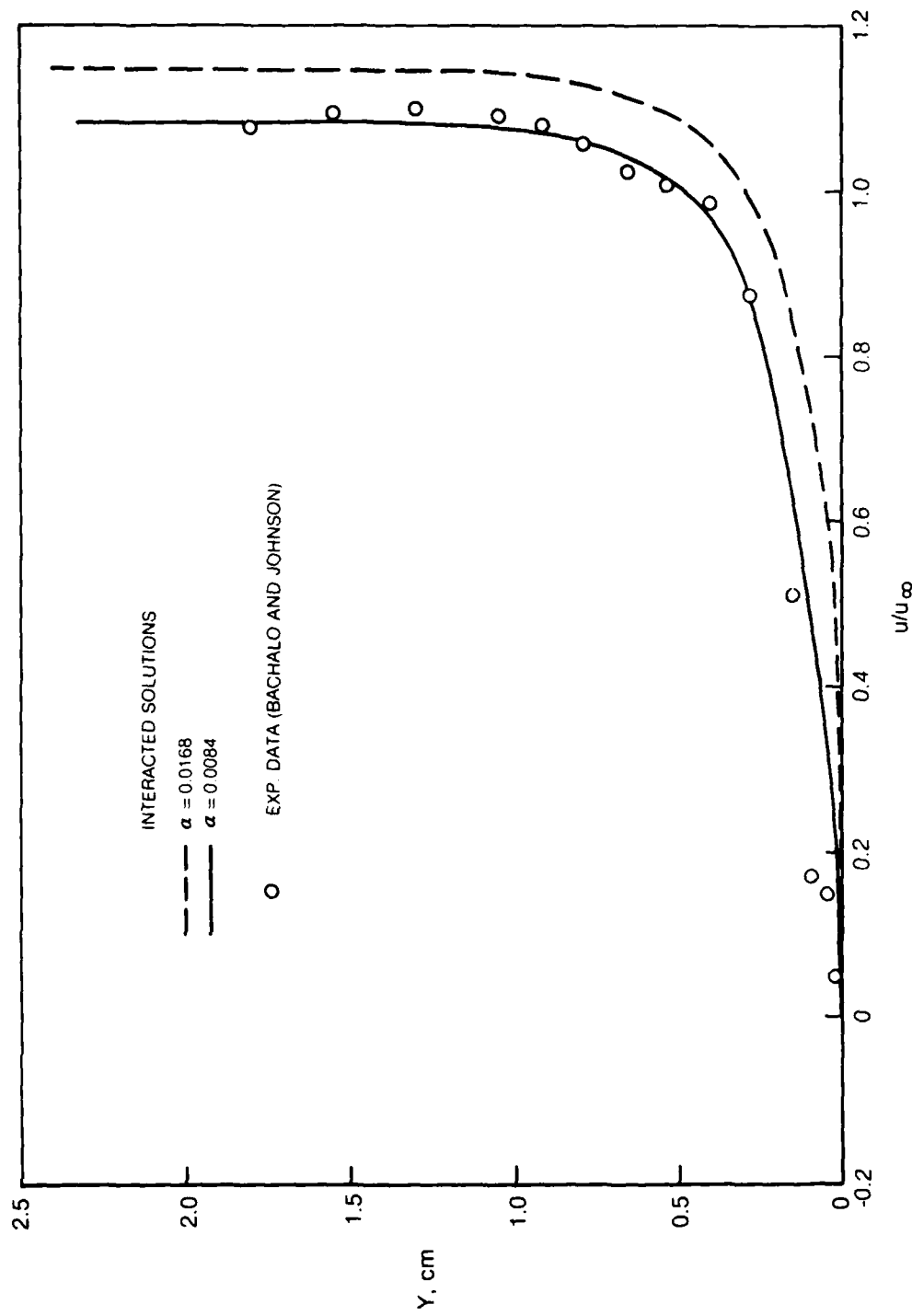
FIG. 14

SKIN FRICTION DISTRIBUTIONS

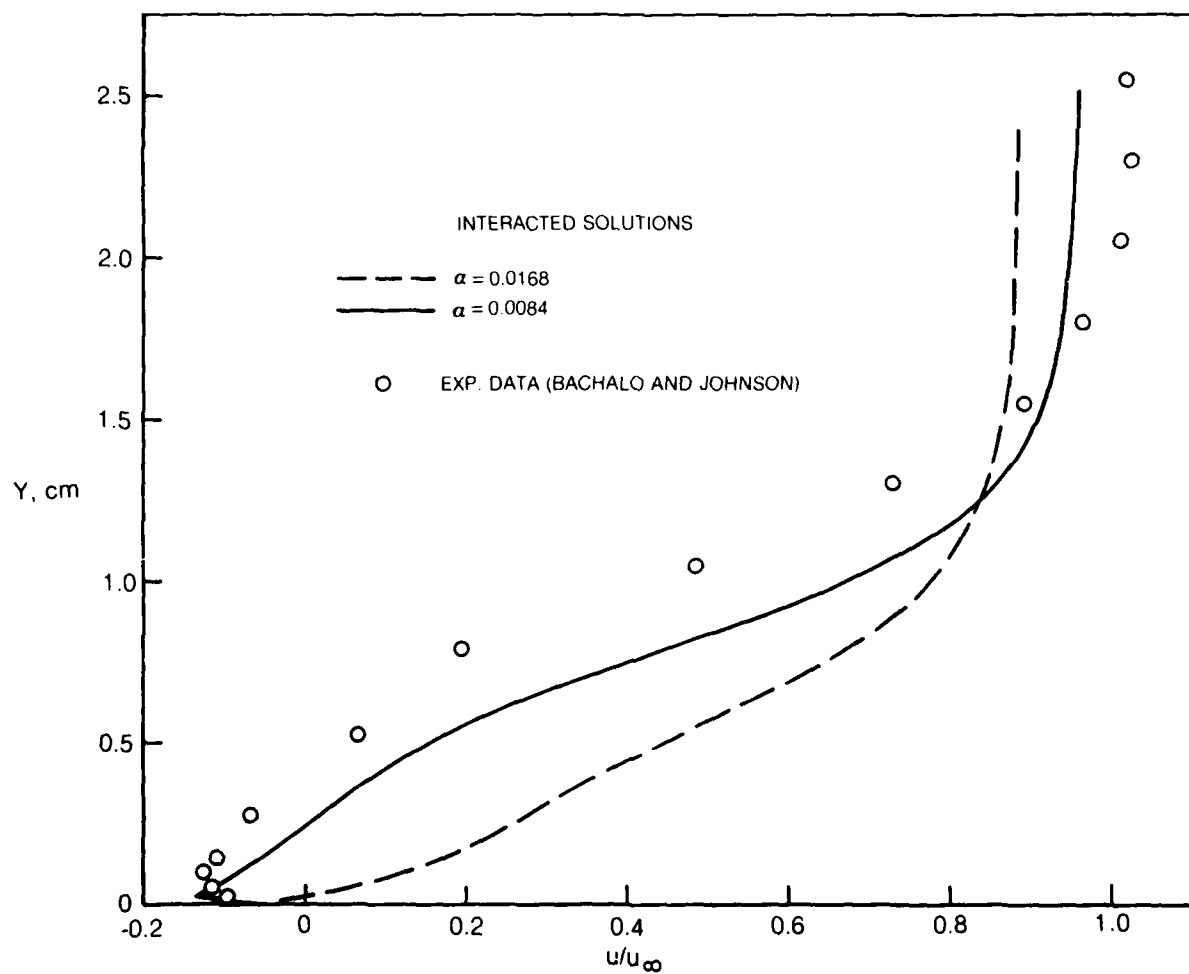


80-11-90-1

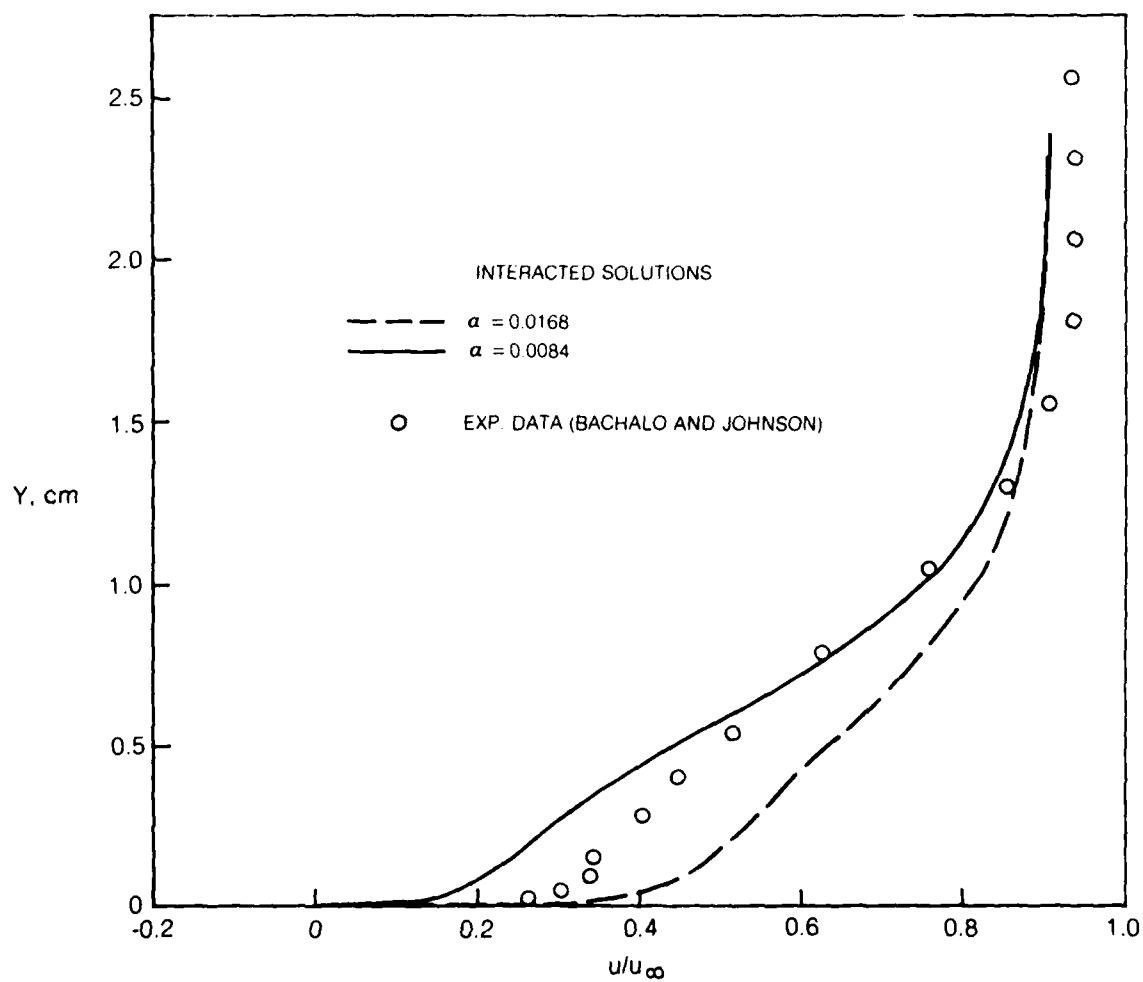
VELOCITY DISTRIBUTIONS

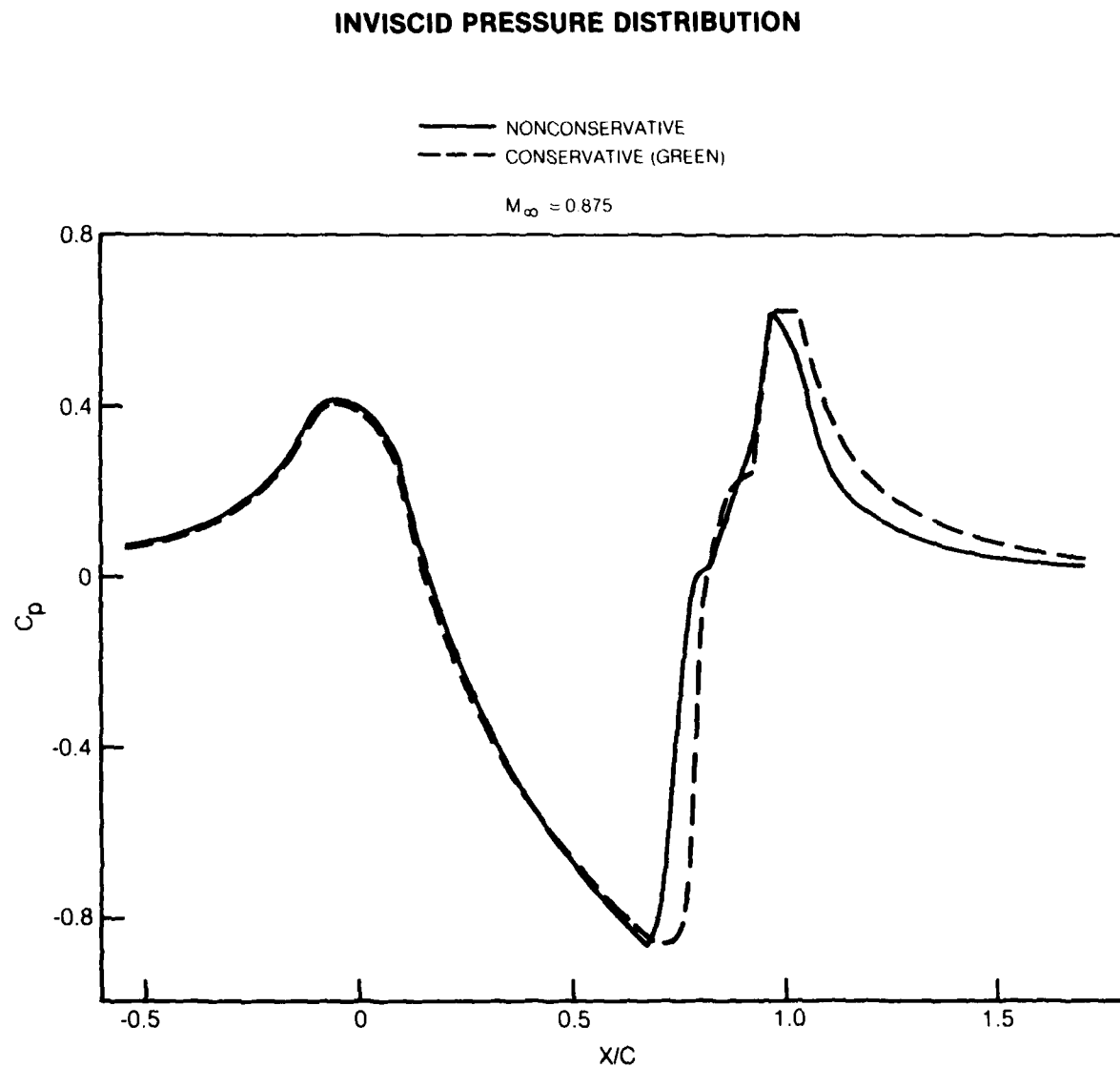
a) $X/C = 0.750$ 

VELOCITY DISTRIBUTIONS (CONTINUED)

b) $X/C = 1.0$ 

VELOCITY DISTRIBUTIONS (CONTINUED)

c) $X/C = 1.25$ 



**DATE
ILMED
— 8**